SILENT STIMULATION OF CONES: A COMPARISON BETWEEN THE ERG AND PLR RESPONSES

Giovanni Gibertoni[a], AB. Pothadia Irungovel[b], Suresh Viswanathan[b], and Luigi Rovati[a]

[a]University of Modena and Reggio Emilia, Department of Engineering "Enzo Ferrari" Via P. Vivarelli 10, 41125 Modena, Italy
[b]SUNY College of Optometry, 33 W 42nd St, NY 10036 New York, United States

ABSTRACT

The Electroretinogram measures the overall electrical activity of the retina in response to light stimulation, while the dynamics of Pupillary Light Reflex reveal information about how the visual pathway innervates the iris muscles in response to such stimuli. By simultaneously evaluating PLR and ERG responses, a deeper understanding of both image-forming and non-image-forming mechanisms of the human visual system can be gained. Additionally, ERG and PLR responses to bursts of light are contributed by all primary classes of photoreceptors, including rods, (L-M-S) cones, and intrinsically photosensitive ganglion cells (ipRGCs). This study presents and tests a low-cost, Maxwellian view-based optical setup that can be used to acquire synchronous PLR and ERG recordings with silent stimulation techniques on cones photoreceptors in human subjects.

Keywords: Pupillary Light Reflex, Electroretinogram, Silent Substitution, Ophthalmic Instrumentation, Ophthalmic Imaging, Biomedical Instrumentation, Optical Measurement Methods, Ophthalmic Measurements

1. INTRODUCTION

The Electroretinogram (ERG)[1,2] is a measurement of the retina's overall electrical activity in response to light stimulation, while the Pupillary Light Reflex (PLR)[3,4] is the process that mediates changes in the pupil area in response to variations in illuminance. ERG techniques, such as full-field flash ERG (ffERG), pattern ERG (PERG), and multifocal ERG (mfERG), are commonly used to evaluate the functional status of the retina and retina-related disorders in human care, veterinary procedures, and medical research.[1,5] On the other hand, Pupillary Light Reflex (PLR) not only provides information about the retina's functional status but also provides insight into both the parasympathetic and sympathetic divisions of the autonomic nervous system, as well as intracranial and neurological connections.[6] ERG and PLR responses to diffuse flashes of light include contributions from all major classes of cones (long-(L), middle-(M), and short-(S) wavelength sensitive photopigment) and rod photoreceptors.[7] While such stimuli are effective in assessing retinal function in a non-selective, global fashion, there is also a lot of interest in recording ERG and PLR that reflect the activity of particular photoreceptor populations.[8,9] However, it can be challenging to stimulate specific photoreceptors without activating others due to the overlap in photopigment spectral sensitivities.[10,11] The Silent Substitution technique is a method that can be used to selectively stimulate specific photoreceptor populations by relying on the "Principle of Unvariance",[12] which asserts that the photocurrent of a specific photoreceptor is only a scalar output and cannot differentiate between changes in wavelength and changes in intensity.

This paper presents a study that combines ERG and PLR silent stimulation techniques to investigate the health and function of the eye and the optic nerve, which can be used to diagnose and monitor eye diseases such as glaucoma, retinitis pigmentosa, and age-related macular degeneration.[13] The paper is organized as follows: in Section 2, the theoretical background of the Silent Substitution technique is briefly discussed. Section 3 provides a description of the experimental setup and the methodology used for preliminary tests carried out on human volunteers. In Section 4, the obtained results are briefly reported and in Section 5, some final considerations and future works are discussed.

2. SILENT SUBSTITUTION TECHNIQUE

The retina's photoreceptors, including rods, cones (Long, Medium, and Short-wavelength sensitive), and ipRGCs, respond differently to different wavelengths of light stimuli.[11] These photoreceptors are responsible for both image-forming functions (mainly rods and cones) and non-image-forming functions (ipRGCs).[14] They all contribute to essential functions of the human-visual system,[14] as well as other behavioral and physiological responses to light in the environment, as they express different proteins, namely *opsins*.[15] Rods express *rhodopsin*, cones express three different types of *photopsin* for the three different wavelength-sensitive classes, and ipRGCs express *melanopsin*. The opsins are responsible for the light-sensitivity of each photopigment[15] and report different peak wavelengths sensitivities.[16,17] In Figure 1b, the cyanopic (S-cones), melanopic, rhodopic, chloropic (M-cones) and erythropic (L-cones) sensitivity curves are shown, from left to right, respectively.[18]

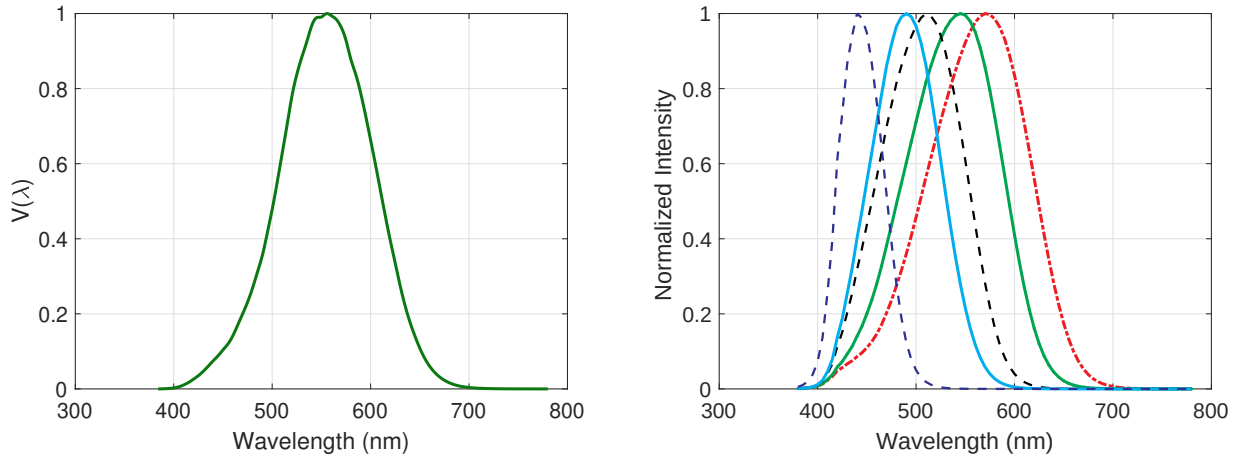

(a) (b)

Figure 1: CIE 10-degrees physiologically-relevant or photopic luminous efficiency function a). Normalized photoreceptors sensitivity curves together with ipRGCS cells sensitivities. From left to right, cyanopic, melanopic, rhodopic, chloropic and erythropic sensitivities b).[18]

Despite the peaks of the photoreceptor's sensitivity curves being spectrally distinct and far away from each other, it is reasonable to consider them as partially overlapping Gaussian distributions.[19] One consequence of this overlap is that the responses of photoreceptors are largely non-specific, thus being color-blind and weighting the input light by means of spectral sensitivity only. Indeed, they do not distinguish between two light stimuli having different intensities or different peak wavelengths.[12,19] This may seem like a major challenge when trying to target a specific type of photoreceptor. Nevertheless, by utilizing the unique properties of the photoreceptors, it is possible to use different combinations of light spectra to stimulate changes in just one photoreceptor while keeping the others unchanged. Indeed, in this way, the effect on that specific photoreceptor can be estimated.[20] Given a specific intensity spectral distribution of the light stimuli, each photoreceptor's stimulation level can be recovered by means of their equivalent illuminance, namely cyanopic, melanopic, rhodopic, chloropic, and erythropic illuminance. Lucas et al. referred to this quantity as *equivalent α-opic illuminance* E_α (α-lux), where α can be one of the five aforementioned photo-sensitives cells.[16] Thus, E_α can be expressed as follows:

$$E_\alpha = K_m \cdot \int E_{e,\lambda}(\lambda) \cdot N_\alpha(\lambda) d\lambda \cdot \frac{\int V(\lambda) d\lambda}{\int N_\alpha(\lambda) d\lambda}, \tag{1}$$

where λ is the radiation wavelength, $K_m = 683.000\, lm/W$ is the maximum spectral luminous efficacy*, $V(\lambda)$ is the normalized spectral luminous efficacy function for the photopic vision (see Fig. 1a), $E_{e,\lambda}$ is the spectral power distribution of the light source (W/m^2), and N_α is the considered photoreceptor sensitivity curve with

*CIE S017:2020 -17-21-092

unity-area normalization.
The aforementioned statement makes the selection of the primary light sources' peak wavelength, i.e. spectral conformation of any possible $E_{e,\lambda}$, a crucial part in the employment of Silent Substitution.[21] Therefore, when a pair of colors or two different light distributions $E_{A,\lambda}(\lambda)$ and $E_{B,\lambda}(\lambda)$ is considered, each photo-sensitive cell is stimulated with of a determined amount or contrast when these colors are alternated.[19,22] In this case, the commonly used Michelson Contrast (C_M), can be computed as follows:[23]

$$C_M = \frac{E_{\alpha-max} - E_{\alpha-min}}{E_{\alpha-max} + E_{\alpha-min}}, \tag{2}$$

where $E_{\alpha-max}$ and $E_{\alpha-min}$ are the maximum and minimum equivalent $\alpha-opic$ illuminances given by the two considered spectral distributions $E_{A,\lambda}(\lambda)$ and $E_{B,\lambda}(\lambda)$ with respect to the specific α photopigment considered. Higher contrast between the two selected colors implies a higher activation of a given photopigment, therefore an increased contribution of its specific effect on the observed phenomena, i.e. PLR or ERGs responses.

2.1 System Optimization

As previously described, the Silent Substitution technique foresees the combination of different primary intensities to achieve a *target* stimulation level in terms of contrast for each photosensitive cell.

As we furtherly describe later in Section 3.1, the system considered for this test case is constituted by four different primaries: Blue (468 nm), Green (523 nm), Yellow (593 nm), and Red (625 nm). The light intensity of each primary, in terms of radiant flux (W), accordingly to our driving technique,[24,25] is proportional to the LED's forward current I_F and therefore to the Duty Cycle (DC $\in [0-100\%)$ used to activate the specific source. To improve the accuracy of the generated light stimuli, we performed a calibration of the system by measuring the output beam radiant flux (W) with an optical power meter 1918R model by Newport (Irvine, CA, USA) with *918d-uv-od3* optical head [†] at different DC levels (10%, 20%, 30%, 50%, 100%). Following, is possible to linearize the conversion from the digitally configured DC value ($[0-100\% \pm 0.1\%]$) to the output radiant flux in Watts by means of a linear fit of the previously measured values with the intercept fixed to 0 (i.e. 0% (DC) = 0 Watts). Moreover, by using the spectral distribution of the LED sources, measured with the Hamamatsu PMA-11 photo-spectrometer (located in Hamamatsu City, Shizuoka, Japan), it is possible to analytically compute the spectral power distribution of each light source, i.e. $E_{e,\lambda}(\lambda)$ (see Eq. 1), for each DC value.

If the contribution of Rods is neglected, thus considering only photopic illumination condition, it is possible to approximate the input-output relation of our four-primaries light source system (RGBY) as a linear set of equations, where the conversion from Duty Cycle (DC) value (i.e. Red, Green, Yellow, and Blue in our case) and the four corresponding $\alpha - opic$ stimulations levels in (α-lux) can be determined by 16 real coefficients, namely $K_{i,j}$, with the following equation:

$$\begin{bmatrix} E_{cyan} \\ E_{mel} \\ E_{chlor} \\ E_{eryth} \end{bmatrix} = \begin{bmatrix} K_{1,1} & K_{1,2} & K_{1,3} & K_{1,4} \\ K_{2,1} & K_{2,2} & K_{2,3} & K_{2,4} \\ K_{3,1} & K_{3,2} & K_{3,3} & K_{3,4} \\ K_{4,1} & K_{4,2} & K_{4,3} & K_{4,4} \end{bmatrix} \times \begin{bmatrix} R_{DC} \\ G_{DC} \\ B_{DC} \\ Y_{DC} \end{bmatrix} \tag{3}$$

Where $R_{DC}, G_{DC}, B_{DC}, Y_{DC}$ are the duty cycle values [0,100%] of Red, Green, Blue, and Yellow LEDs used in our system. $E_{cyan}, E_{mel}, E_{chlor}, E_{eryth}$ are the equivalent α-opic illuminance for Cyan-opic (S-cones), Melan-opic (ipRGCs), Chlor-opic (M-cones), and Erythr-opic (L-cones), respectively. For any pair of colors (**A** and **B**), i.e. eight pairs of DC values, it is possible to compute the stimulation levels for each photopigment with the above equation. The Michelson Contrast (C_M) for any given photopigment activation level delivered by switching from the two given colors **A** and **B** can be calculated with Eq. 2. Finally, we used a Generalized Reduced Gradient[26] (GRG) algorithm to optimize and find the best combination of DC values to achieve a target contrast on a specific photopigment while silencing the others.

[†] https://www:newport:com/ p/918D-UV-OD3R

3. MATERIALS AND METHODS

In this section, the design of the instrumentation and the measurement procedures are presented. Specifically, the experimental setup based on Silent Substitution is described in Section 3.1. The test methodology, including technical information about the light spectral distribution and stimulation timing, is presented in Section 3.2.

3.1 System Setup

In this work, a Maxwellia-View[27] based optical system is used to simultaneously record PLR and ERG responses under the silent stimulation of cones for human subjects. The device used for this experiment is an upgraded version of the monocular pupillometer presented in our previous work, *"A simple Maxwellian optical system to investigate the photoreceptors contribution to pupillary light reflex"*.[24] The device schematic diagram, depicted in Figure 2, consists of a double-lens optical scheme that includes four fiber-coupled high-brightness BGRY LED light sources and a board-level 6.4 MPx CMOS camera, that is used to acquire grayscale images of the human eye. As described in,[24,28] the optical design of the instrument presents several advantages in the field of pupillometry. In particular, the simple-two lenses stage, which achieves Maxwellian-View, allows superior control of the light stimulation intensity on the retina while avoiding the utilization of pupil dilation practices.

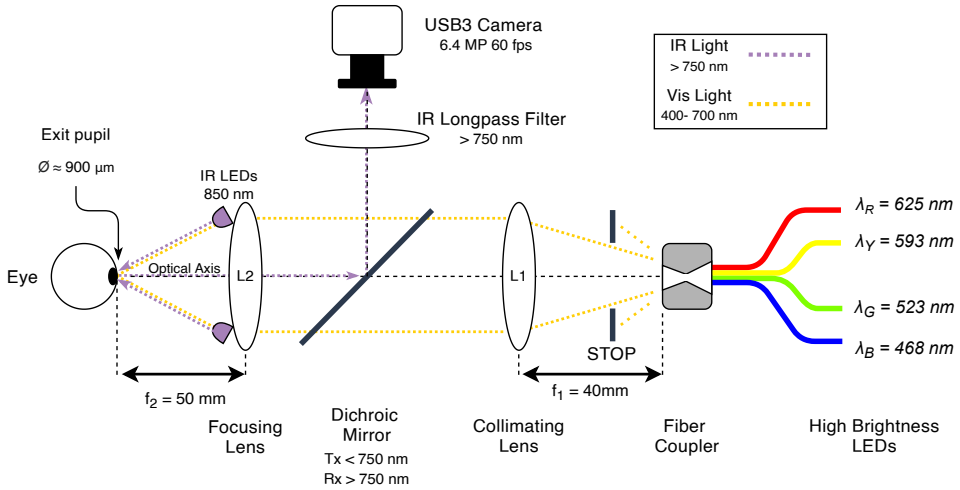

Figure 2: Optical diagram of the *Pupillary Light Reflex* instrument[24] used to collect data. *Infra-Red Light* optical path (dash purple line), i.e. *acquisition path*, allows eye recording while eye stimulation is achieved trough *Visible Light* optical path (dashed yellow line). Lens **L1** ($f_1 = 40mm$, $D_1 = 2.54cm$) together with a stop aperture has been used to collimate the light towards lens **L2** ($f_2 = 50mm$, $D_2 = 2.54cm$) that focuses the light beam to the eye's pupil plane, obtaining an output spot-size of $\approx 900\ \mu m$ diameter with a full-width viewing angle $\theta = 20.5°$.

Moreover specifically, the optical design provides a focused beam with a diameter of 900 um and a 20-degree field of view. The infrared-sensitive CMOS camera has been used together with eight 850 nm infrared LEDs circularly arranged around the lens **L2** and a high-pass optical filter (see. Fig. 2) to acquire pupil responses up to 60 Hz.

ERGs were measured from the dominant eye using a silver/nylon corneal fiber electrode[‡] (DTL Plus Electrodes, Diagnosys LLC in Lowell, MA, USA) as the reference and a 9mm Ag/AgCl electrode (from Biosense Medical in Chelmsford, UK) on the earlobe as the ground. The impedance was kept below 5 $k\Omega$. The signals were recorded using the Espion E2 system and Espion (v6.64) software from Diagnosys(Lowell, MA, USA), which amplified and filtered the ERGs with a bandwidth of 1 Hz to 300 Hz and digitized them at a rate of 1000 Hz.

The device timing, thus including light stimulation, frame acquisition, and ERGs recording is controlled by a microcontroller unit (MCU)[§] with a 32-bit ARM core a and 80 MHz clock frequency. Additionally, a user-

[‡]https://www.diagnosysllc.com/product/dtl-plus-electrodes/
[§]Atmel SAM3X8E ARM Cortex-M3

friendly interface made with NI LabVIEW[¶] is used to configure light stimulation and acquisition settings and allows monitoring of the experiment in real-time.

3.2 Test Methodology

Four experiments, stimulating the two different classes of cones photoreceptors (L and S) singularly with two different contrast (C_M) while silencing the others along with ipRGCs, have been carried out on three male volunteers (S1, S2, and S3) aged 24, 34, and 55 years old. The experiments have been carried out in a controlled illumination environment, where a series of 200 ms flashes were presented with a 0.5 Hz frequency or 2 seconds period. This timing configuration has been specifically selected as a trade-off between clear ERGs and PLR responses. As we can learn from the literature the easiest way to get clear ERGs responses is by repeating many high-brightness short flashes (duration ¡ 100 ms)[29] at 2-3 Hz interval frequency. Differently, for well-visible pupil responses, longer flashes, in the range of 500 ms or more[30,31] with much higher interval time, i.e. in the range of seconds, are preferable. In our case, since both signals are recorded at the same time, timing values that will work for both techniques must be considered. Therefore, as the best compromise between clear and meaningful responses and test duration, the timeline depicted in Figure 3 has been used in all four of our experiments.

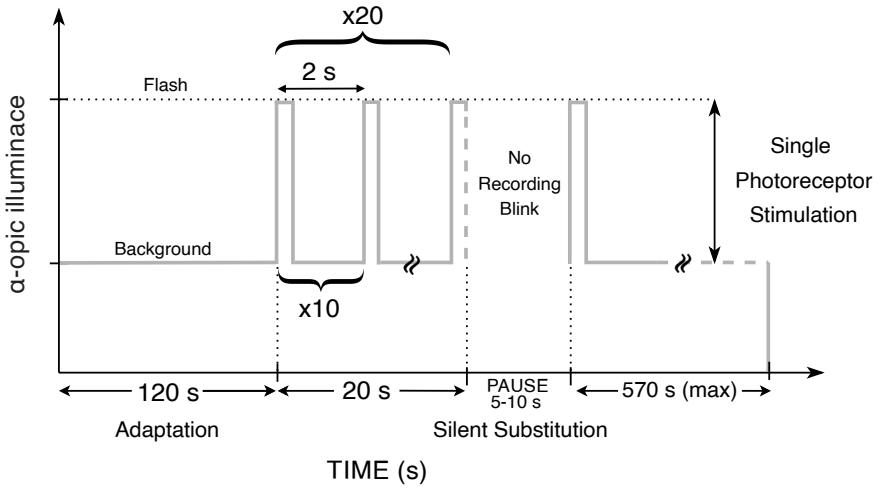

Figure 3: Experimental temporal phases: (i) 120 seconds of background *adaptation* in a controlled environment, (ii) single photoreceptor stimulation ($\approx$ 10 min). During the stimulation phase, 200 ms light flashes with higher equivalent illuminance for one selected photoreceptor with respect to the background illumination are presented with a interleave period of 2 seconds. Every 10 flashes (20 s) a *PAUSE* interval with a variable duration comprised between 5 and 10 s is used to allow the patient to blink.

More specifically, for each experiment, we used a 2 minutes *adaptation phase (i)* with background illumination, while natural eye-blink was allowed. During this phase, only the recording of pupil size was active to evaluate the subject's specific pupil size at the background illumination level. Afterward, the stimuli were presented in a series of 10 consecutive flashes for a total of 20 seconds where no blinks were allowed since ERGs signals are extremely sensitive even to the smallest ciliary muscle movements. The *stimulation phase (ii)* is followed by a *PAUSE* interval with a variable duration comprised between 5 and 10 seconds to allow the subject to blink and rest for the next series of flashes. The 10 flashes stimulation phase with pause interval is then repeated up to 20 times, for a total of 200 averages of single burst responses. During the 20 seconds stimulation phase, the simultaneous recording of both ERG and PLR responses is active on the stimulated eye, while during the pause no recording is active except for the live video stream that allows for continuous adjustment of the eye alignment performed by the operator.

Accordingly to the silent substitution technique presented in Section 2, we optimized the LED intensity for each experiment to obtain a *target* Michelson Contrast C_M (see. Eq. 2) of 40% $\pm$ 2% and 70% $\pm$ 2%

[¶]https://www.ni.com/en-us/shop/labview.html

for L-CONEs (experiments #1 and #2) and S-CONES (experiments #3 and #4). Table 1 summarize all the specifications of the light stimuli for each experiment. The *Base* columns refer to the background stimulation level, while *Flash* columns highlight the specifications with increased stimulation on the specified photopigment.

Table 1: Experiments specification. The $\alpha - opic$ stimulation levels reported as **B, M, G, R** are indicative for Cyan-opic (S-cones, **B**lue), **M**elan-opic (ipRGCs), Chlor-opic (M-cones, **G**reen), and Erythr-opic (L-cones, **R**ed), respectively. Red highlighted cells show the increment of equivalent $\alpha - opic$ activation on the *target* photopigment.

		Experiment #1 L-CONE 40% C_M		**Experiment #2 L-CONE 70% C_M**		**Experiment #3 S-CONE 40% C_M**		**Experiment #4 S-CONE 70% C_M**	
		Base	**Flash**	**Base**	**Flash**	**Base**	**Flash**	**Base**	**Flash**
Perceived Color		Orange	Red	Green	Red	Dark Yellow	Pink	Light Green	Pink
Wavelengths (nm)		-	-	473	473	473	-	473	437
		531	-	531	-	531	473	530	530
		595	595	595	-	-	595	-	595
		-	630	-	630	630	-	630	630
Total Radiant Flux (uW)		0.80	3.38	0.64	5.59	1.26	1.41	1.62	1.72
Luminance (cd/m2)		88.42	163.29	73.37	264.64	105.19	89.92	149.22	130.91
α**-opic illuminance (α-lux)**	**B**	0.07	0.09	0.39	0.71	1.34	3.08	0.56	3.06
	M	0.55	0.22	2.11	1.06	3.61	3.99	3.95	4.77
	G	2.84	2.90	3.15	4.87	4.22	3.81	5.93	5.29
	R	3.97	9.03	2.78	14.7	4.49	4.43	5.92	6.10
FOV		20.5 ° FOV							
Number of subjects		3 Males (age 23,34,53)							
Timing		200 ms flash with 2 seconds period (10 flash seq.)							
Test Condition		Afternoon – Room light – Undilated Eye							
Averages		100 to 200 recordings on the same day for each subject							

As highlighted in the Table, the four experiments share the same viewing angle (FOV), timing, and environmental condition. The number of averages recorded for each experiment and subject was closely linked to the noise level of ERGs signals and ranged from 100 to 200 for all tests. For completeness, Figure 4 shows the whole spectra flux distributions (W/m^2) in the visible range used for each experiment.

4. PRELIMINARY RESULTS AND DISCUSSION

By using silent substitution, isolating the responses of L and S Cones were made possible along with measuring simultaneous PLR and ERG signals to those specific stimuli. In Section 4.1, we present the results described by ERGs signals while, in Section 4.2, the results concerning PLR responses are shown.

4.1 ERG results

Figures 5a,5b, and 5c highlight characteristics of the ERG's isolated responses for L and S cone silent stimulation at 40% and 70% C_M on the three subjects, namely S1, S2, and S3 respectively. Time t = 0 s corresponds to the beginning of the 200 ms flash for all the graphs. As previously mentioned, each curve represents the average from over 100 single flash responses. After averaging, the responses have been band-pass filtered with [1 Hz - 300 Hz] cutoff frequencies accordingly to ISCEV's last dated guide to electroretinography[29,32] and to other reference research studies.[10,33] Moreover, we performed smoothing with cubic spline,[34] while keeping the total attenuation of the signal under 3%. Statistics of ERGs average responses from the three subjects are reported in Table 2.

As can be seen in Fig. 5, ERGs individual responses are pretty consistent for the three subjects. In particular, we can notice that the amplitudes of a-wave, b-wave, and d-wave,[1] as well as for the *photopic negative response* (PhNR)[35] are higher for the L-CONEs (dashed dark red line in Fig. 5) with 70% C_M, thus for all the three subjects (See Table 2). The L-CONEs 40% C_M instead (solid orange line), show lower values in terms of PhNR (-4.46 μV) and *OFF-Response*, or d-wave, which is what is normal to be expected from lower intensity (i.e. lower contrasted) flashes.[36] Looking at the S-Cones responses, a different trend from L-Cones is appreciable for all

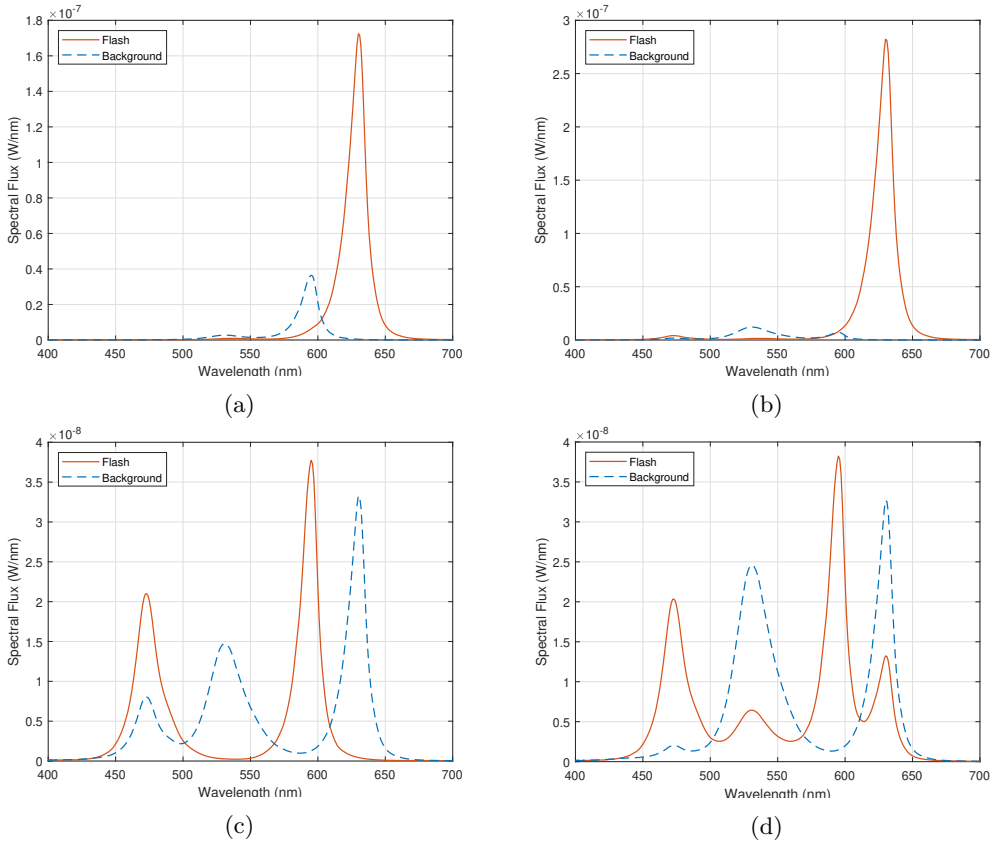

Figure 4: Spectral distribution of light stimuli used for the silent substitution in the four experiments. For each graph, the blue dashed line is the background spectrum while the orange solid line is the spectral flux used as a flash for each test. a) shows spectral flux for experiment **#1** with 40% contrast on L-cones (RED), b) shows the experiment **#2** with 70% contrast on L-cones, c) shows experiment **#3** with 40% contrast on S-cones (BLUE), and d) shows experiment **#4** with 70% contrast on S-cones.

three subjects. In particular, b-wave and PhNR amplitudes are lower for both S-Cones 40% and 70% contrast, especially for subject S1 (Fig. 5a) and S3 (Fig. 5c) if compared to the L-Cones counterpart. Taking a closer look, b-waves for S-Cones at 70% C_M also show to be slightly delayed (48.32 ms) if compared to the 40% ones (40.69 ms). Moreover, S-Cones shows a significantly lower amplitude (2.250 - 2.406 μV) and delayed (337 - 365 ms) d-wave (OFF-Response) if compared to L-Cones (3.745 - 12.485 μV) amplitudes and (243 - 297 ms) d-wave specifications.

Table 2: Average ERGs response statistics

Cones Type	a-wave time (ms)	a-wave amplitude (uV)	b-wave time (ms)	b-wave amplitude (uV)	PhNR-wave time (ms)	PhNR-wave amplitude (uV)	d-wave time(ms)	d-wave amplitude (uV)
L-CONE 70% C_M	16.59	-0.846	42.06	4.285	105.89	-9.378	297	12.485
L-CONE 40% C_M	18.94	-0.924	46.09	2.933	86.68	-4.461	243	3.745
S-CONE 70% C_M	19.84	-0.995	48.32	1.491	130.92	-2.949	365	2.406
S-CONE 40% C_M	16.57	-0.389	40.69	1.501	98.11	-3.587	337	2.250

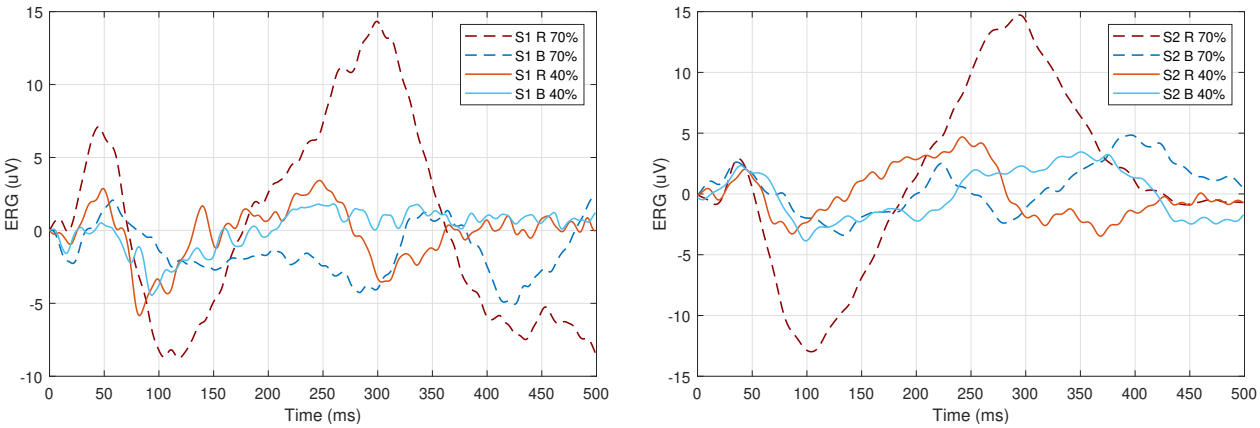

(a) (b)

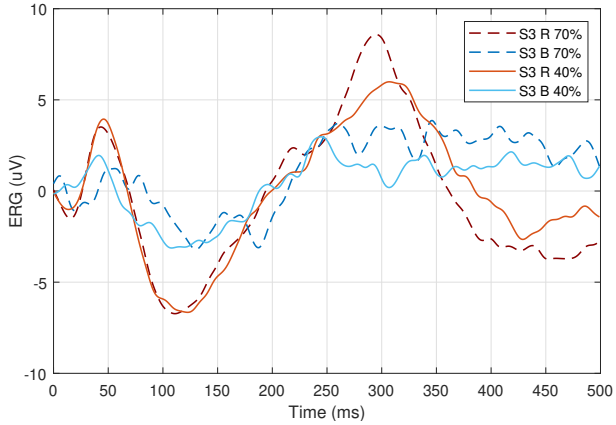

(c)

Figure 5: ERGs electrical response to L and S cones silent stimulation. (a), (b), and (c) refers to subjects S1, S2 and S3, respectively. Dashed dark red lines (R 70%) correspond to L-Cones stimulation at 70% C_M; Solid orange lines (R 40%) to L-Cones stimulation at 40% C_M; Dashed blue lines (B 70%) to S-Cones stimulation at 70% C_M; Solid light blue lines (B 40%) to S-Cones stimulation at 40% C_M. For all graphs, time t=0 ms corresponds to the beginning of the 200 ms flash.

4.2 PLR results

PLR responses have been simultaneously recorded with ERG as explained in Section 3, where single flash responses have been averaged for each subject. The point-by-point averaged responses of each subject, have been furtherly normalized accordingly to the following equation:

$$\overline{P_D}(t) = 100 \cdot \frac{P_D(t) - min(P_D)}{P_D(t = t_0) - min(P_D)} \tag{4}$$

Where $\overline{P_D}(t)$ is the pupil diameter normalized value at time t, $P_D(t)$ is the pupil diameter at time t in mm, $min(P_D)$ is the minimum size of the pupil diameter in mm and $P_D(t = t_0)$ is the pupil diameter in mm a time $t = 0$, i.e. just before the beginning of the flash. This normalization technique allows us to furtherly average the responses among the three subjects, thus enhancing timing and the recovery phase as explained in our previous articles.[24] Figure 6 shows the average combined responses for L and S cone silent stimulation at 40% and 70% C_M among the three subjects.

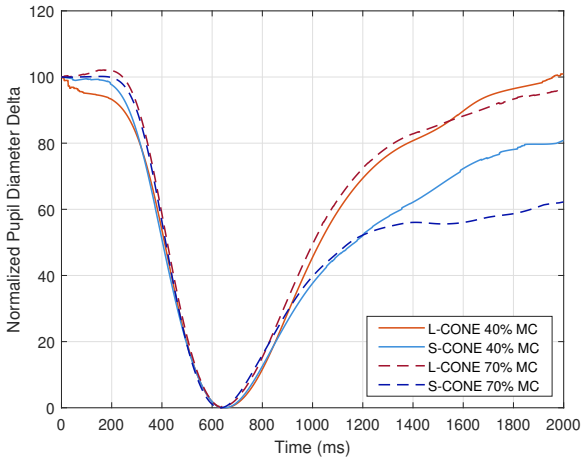

Figure 6: Normalized and averaged PLR response among the three subjects for 200 ms flash-driven response. Time t=0 ms corresponds to the beginning of the 200 ms flash.

As shown in Figure 6 and reported in Table 3, there is a noticeable difference in the recovery phase of PLR between S-Cones (solid light-blue line and dashed blue line) and L-CONES (dashed red line and solid orange line). Specifically, the average S-CONEs induced PLR response recovers to 80% for 40% C_M and 60% for 70% C_M of the initial background-adapted diameter. This is further confirmed by the data in Table 3, which shows that the PLR dilation time constant for L-Cones is around 500 ms, while it is 50% higher for 40% S-Cones at 764 ms and 100% higher for 70% S-Cones at over 1000 ms (Refer to[24] for more information on PLR dilation time constant).

Table 3: Average PLR waveforms values for 200 ms flashes at 40% and 70% Michelson Contrast

Cones Type	**Constriction Delay (ms)**	**Peak Constriction Time (ms)**	**Constriction Time (ms)**	**Dilation Time Constant (ms)**
L-CONEs 70% C_M	291	638	305	509
L-CONEs 40% C_M	260	652	379	500
S-CONEs 70% C_M	287	632	296	1035
S-CONEs 40% C_M	256	651	339	764

5. CONCLUSIONS

In this study, we demonstrated the effectiveness of using a low-cost Maxwellian-View optical system for Silent Substitution in observing PLR and ERG signals on human subjects. Despite the smaller field of view (20 degrees), the results were repeatable among different subjects and provided simultaneous measurement of the pupil function. Our findings, as shown in Figures 5 and 6 of Section 4, reveal how ERG and PLR responses offer distinct insights into the human visual pathway, with ERG providing more information in the first 300 ms after flash and PLR providing useful knowledge on iris-muscle plant reaction and pupil recovery phase in the time range between 200-2000 ms. This approach proved to be a faster, less invasive, and more comprehensive way of investigating and potentially detecting common optic-nervous system disorders. We plan to expand this research by conducting a measurement campaign on humans affected by mild traumatic brain injury (mTBI) in future experiments.

REFERENCES

[1] Perlman, I., [*The Electroretinogram: ERG*], University of Utah Health Sciences Center, Salt Lake City (UT) (1995).

[2] McAnany, J. J., Park, J. C., Fishman, G. A., and Collison, F. T., "Full-Field Electroretinography, Pupillometry, and Luminance Thresholds in X-Linked Retinoschisis," *Investigative Ophthalmology & Visual Science* **61**, 53 (June 2020).

[3] Kardon, R., "Pupillary light reflex," *Current opinion in ophthalmology* **6**, 20–26 (Dec. 1995).

[4] Heller, P. H., Perry, F., Jewett, D. L., and Levine, J. D., "Autonomic components of the human pupillary light reflex.," *Investigative Ophthalmology & Visual Science* **31**, 156–162 (Jan. 1990).

[5] Marmoy, O. R. and Viswanathan, S., "Clinical electrophysiology of the optic nerve and retinal ganglion cells," *Eye* **35**, 2386–2405 (Sept. 2021). Number: 9 Publisher: Nature Publishing Group.

[6] Usui, S. and Stark, L., "A model for nonlinear stochastic behavior of the pupil," *Biological Cybernetics* **45**, 13–21 (Aug. 1982).

[7] Zhang, F., Kurokawa, K., Lassoued, A., Crowell, J. A., and Miller, D. T., "Cone photoreceptor classification in the living human eye from photostimulation-induced phase dynamics," *Proceedings of the National Academy of Sciences of the United States of America* **116**, 7951–7956 (Apr. 2019).

[8] Viénot, F., Bailacq, S., and Rohellec, J. L., "The effect of controlled photopigment excitations on pupil aperture," *Ophthalmic and Physiological Optics* **30**(5), 484–491 (2010). _eprint: https://onlinelibrary.wiley.com/doi/pdf/10.1111/j.1475-1313.2010.00754.x.

[9] Zele, A. J., Adhikari, P., Cao, D., and Feigl, B., "Melanopsin and Cone Photoreceptor Inputs to the Afferent Pupil Light Response," *Frontiers in Neurology* **10**, 529 (2019).

[10] Maguire, J., Parry, N. R. A., Kremers, J., Murray, I. J., and McKeefry, D., "Human S-cone electroretinograms obtained by silent substitution stimulation," *JOSA A* **35**, B11–B18 (Apr. 2018). Publisher: Optica Publishing Group.

[11] Cie, "CIE S 026/E:2018 CIE System for Metrology of Optical Radiation for ipRGC-Influenced Responses to Light," tech. rep., International Commission on Illumination (CIE) (Dec. 2018).

[12] Rushton, W. A. H., Powell, D. S., and White, K. D., "Exchange thresholds in dichromats," *Vision Research* **13**, 1993–2002 (Nov. 1973).

[13] Feigl, B. and Zele, A., "Melanopsin-expressing intrinsically photosensitive retinal ganglion cells in retinal disease," *Optometry and vision science : official publication of the American Academy of Optometry* **91** (05 2014).

[14] Berson, D. M., "Strange vision: ganglion cells as circadian photoreceptors," *Trends in Neurosciences* **26**, 314–320 (Jun 2003).

[15] Terakita, A., "The opsins," *Genome Biology* **6**, 1–9 (Mar 2005).

[16] Lucas, R. J., Peirson, S. N., Berson, D. M., Brown, T. M., Cooper, H. M., Czeisler, C. A., Figueiro, M. G., Gamlin, P. D., Lockley, S. W., O'Hagan, J. B., Price, L. L. A., Provencio, I., Skene, D. J., and Brainard, G. C., "Measuring and using light in the melanopsin age," *Trends in Neurosciences* **37**, 1–9 (Jan. 2014).

[17] Enezi, J. a., Revell, V., Brown, T., Wynne, J., Schlangen, L., and Lucas, R., "A "Melanopic" Spectral Efficiency Function Predicts the Sensitivity of Melanopsin Photoreceptors to Polychromatic Lights," *Journal of Biological Rhythms* **26**, 314–323 (Aug. 2011). Publisher: SAGE Publications Inc.

[18] CIE, S., "Cie international standard (cie s 026/e:2018) "system for metrology of optical radiation for iprgc-influenced responses to light"," *CIE Central Bureau: Vienna, Austria* **26** (12 2018).

[19] Spitschan, M. and Woelders, T., "The Method of Silent Substitution for Examining Melanopsin Contributions to Pupil Control," *Frontiers in Neurology* **0** (2018). Publisher: Frontiers.

[20] Estévez, O. and Spekreijse, H., "The "silent substitution" method in visual research," *Vision Research* **22**, 681–691 (Jan 1982).

[21] Evéquoz, G., Truffer, F., and Geiser, M., "Maximum possible contrast level for silent substitution: a theoretical model applied to melanopsin stimulation," *JOSA A* **38**, 1312–1319 (Sept. 2021). Publisher: Optica Publishing Group.

[22] Patrick, F., Jessica, S., Gilles, E., Pierre, B., and Martial, G., "Homogeneous light stimulation of melanopsin and cones with a Maxwellian view device for the human eye," in [*2021 IEEE International Instrumentation and Measurement Technology Conference (I2MTC)*], 1–5 (May 2021). ISSN: 2642-2077.

[23] Zele, A. J., Adhikari, P., Cao, D., and Feigl, B., "Melanopsin and Cone Photoreceptor Inputs to the Afferent Pupil Light Response," *Frontiers in Neurology* **0** (2019).

[24] Gibertoni, G., Pinto, V. D., Cattini, S., Tramarin, F., Geiser, M., and Rovati, L., "A simple Maxwellian optical system to investigate the photoreceptors contribution to pupillary light reflex," in [*Ophthalmic Technologies XXXII*], **11941**, 52–60, SPIE (Mar. 2022).

[25] Gibertoni, G., *Design and realization of a binocular pupillometer for RGB flicker annoyance estimation*, master thesis dissertation, Università di Modena e Reggio Emilia (Apr. 2019).

[26] Lasdon, L. S., Fox, R. L., and Ratner, M. W., "Nonlinear optimization using the generalized reduced gradient method," *Revue française d'automatique, informatique, recherche opérationnelle. Recherche opérationnelle* **8**(V3), 73–103 (1974). ISBN: 0397-9350 Publisher: EDP Sciences.

[27] Westheimer, G., "The maxwellian view," *Vision Research* **6**, 669–682 (Dec. 1966).

[28] Gibertoni, G., Borghi, G., and Rovati, L., "Vision-Based Eye Image Classification for Ophthalmic Measurement Systems," *Sensors* **23**, 386 (Jan. 2023). Number: 1 Publisher: Multidisciplinary Digital Publishing Institute.

[29] Thompson, D. A., Fujinami, K., Perlman, I., Hamilton, R., and Robson, A. G., "ISCEV extended protocol for the dark-adapted red flash ERG," *Documenta Ophthalmologica* **136**, 191–197 (June 2018).

[30] Fan, X. and Yao, G., "Modeling Transient Pupillary Light Reflex Induced by a Short Light Flash," *IEEE Transactions on Biomedical Engineering* **58**, 36–42 (Jan. 2011).

[31] Yamaji, K., Hirata, Y., and Usui, S., "A method for monitoring autonomic nervous activity by pupillary flash response," *Systems and Computers in Japan* **31**(4), 22–31 (2000). _eprint: https://onlinelibrary.wiley.com/doi/pdf/10.1002/%28SICI%291520-684X%28200004%2931%3A4%3C22%3A%3AAID-SCJ3%3E3.0.CO%3B2-W.

[32] McCulloch, D. L., Marmor, M. F., Brigell, M. G., Hamilton, R., Holder, G. E., Tzekov, R., and Bach, M., "ISCEV Standard for full-field clinical electroretinography (2015 update)," *Documenta Ophthalmologica* **130**, 1–12 (Feb. 2015).

[33] Maguire, J., *The Isolation of Human Rod and Cone Photoreceptor Activity combining Electroretinography and Silent Substitution Techniques*, PhD thesis, University of Bradford (2017).

[34] Craven, P. and Wahba, G., "Smoothing noisy data with spline functions," *Numer. Math.* **31**, 377–403 (Dec. 1978).

[35] Drasdo, N., Aldebasi, Y. H., Chiti, Z., Mortlock, K. E., Morgan, J. E., and North, R. V., "The S-Cone PhNR and Pattern ERG in Primary Open Angle Glaucoma," *Investigative Ophthalmology & Visual Science* **42**, 1266–1272 (May 2001).

[36] Machida, S., "Clinical Applications of the Photopic Negative Response to Optic Nerve and Retinal Diseases," *Journal of Ophthalmology* **2012**, e397178 (Oct. 2012). Publisher: Hindawi.